PERGAMON

Solid-State Electronics 43 (1999) 131–140

SOLID-STATE ELECTRONICS

2D simulation of the effects of transient enhanced boron out-diffusion from base of SiGe HBT due to an extrinsic base implant

Md. R. Hashim, R. F. Lever, P. Ashburn

Department of Electronics and Computer Science, University of Southampton, Southampton, SO17 1BJ, U.K.

Received 12 March 1998; received in revised form 29 May 1998

Abstract

Transient enhanced diffusion of boron in SiGe HBTs is studied by comparing measurements of the temperature dependence of the collector current with the predictions of 2D process and device simulations. The collector current is chosen for modelling because it is extremely sensitive to very small amounts of out-diffusion from the SiGe base, and hence provides a rigorous test for the accuracy of the transient enhanced diffusion models. The SiGe HBT studied incorporates an ion implanted extrinsic base adjacent to the SiGe base, which allows the influence of the implantation damage on the boron diffusion to be studied. The process simulations show that point defects generated by the extrinsic base implant lead to a broadening of the basewidth around the perimeter of the emitter due to transient enhanced diffusion of boron from the SiGe base. This causes parasitic energy barriers to form, which in the worst case, extend laterally several microns from the edge of the extrinsic base. The electrical effect of the transient enhanced diffusion is a decrease in collector current as the emitter geometry is reduced. Transistors with different emitter geometries and undoped SiGe spacer thicknesses are studied and the collector/base reverse bias is varied to modulate the parasitic energy barrier at the collector/base junction. The trends in the measured collector current are in all cases well predicted by a simplified "plus one" transient enhanced diffusion model.
© 1998 Elsevier Science Ltd. All rights reserved.

1. Introduction

The trend in high-speed, silicon bipolar transistors is towards thin, highly doped bases to reduce the base transit time and base resistance and hence produce circuits which operate at high frequencies [1]. This trend can be taken further in a SiGe Heterojunction Bipolar Transistor (HBT), since the increased gain resulting from the narrower base bandgap can be traded for a dramatically increased base doping. Furthermore, the high base doping concentration allows the basewidth to be further reduced without encountering the limit imposed by punch-through of the base. This approach to HBT design has led to transistors with cut-off frequencies as high as 130 GHz [2], maximum oscillation frequencies as high as 160 GHz [3] and ECL gate delays as low as 9.3 ps [4–6].

Device performance such as this is only achievable if out-diffusion of boron from the SiGe base can be avoided. In the majority of SiGe HBT technologies, high temperature heat treatments after the growth of the SiGe layer are either avoided or minimised. From the point of view of CMOS integration, this approach has the advantage that a low thermal budget SiGe HBT can be fabricated at the end of the process without altering the characteristics of the MOS transistors. However, it has the disadvantage of limiting the savings in process complexity that can be achieved by combining MOS and bipolar process steps. An example of such a saving is the *p*-channel source/drain implant, which can also be used to produce the extrinsic base region of the SiGe HBT. This approach has been used to produce a simple, single-polysilicon BiCMOS process which incorporates a SiGe HBT [7].

0038-1101/98/$ - see front matter © 1998 Elsevier Science Ltd. All rights reserved.
PII: S0038-1101(98)00195-6

In a technology such as this, it is important to be able to accurately model transient enhanced diffusion [8–10], because the point defects generated by the extrinsic base implant cause a dramatic enhancement of the boron diffusion coefficient. In fact the relative contribution of non-equilibrium point defects to boron diffusion becomes more important as the anneal temperature is reduced, and hence it is vital to understand the effects of transient enhanced diffusion in devices such as SiGe HBTs where the anneal budgets have to be minimised.

Although considerable research has been carried out on modelling the defect interactions involved in transient enhanced boron diffusion, relatively little has been published on the 2D modeling of these effects in devices. Some work on polysilicon emitter bipolar transistors has been reported [11, 12] in which two-dimensional device modelling was used to study the effects of transient enhanced diffusion in CMOS-compatible silicon bipolar transistors. However, little has been published on similar 2D process and device modelling in SiGe HBTs. The modelling of transient enhanced diffusion in SiGe HBTs offers a severe challenge, since the collector current is extremely sensitive to very small amounts (tens of angstroms) of boron out-diffusion from the SiGe base. Measurements of collector current on SiGe HBTs therefore provide a uniquely sensitive method of detecting small amounts of transient enhanced boron diffusion, and hence provide an effective way of assessing the accuracy of transient enhanced diffusion models.

In this paper, a detailed comparison of measured and simulated collector currents is made on SiGe HBTs over a range of temperatures from 200 to 300 K. The simulated results are obtained by first of all calibrating the transient enhanced diffusion model parameters by comparing measured SIMS profiles with 1D process simulations on buried boron marker layers implanted with a high dose boron extrinsic base implant. 2D process simulation is then carried out to predict the two dimensional boron profile in the SiGe base adjacent to the extrinsic base. The resulting 2D doping profiles are finally fed into a 2D device simulator, which is used to predict the temperature dependence of the collector current for comparison with measurement. Measured and simulated characteristics are compared for devices with different undoped SiGe spacer thicknesses and different geometries. It is shown that a simple "plus one" transient enhanced diffusion model is able to predict both the measured collector current as a function of temperature and the geometry dependence of the collector current.

2. Simulation procedure

Fig. 1 shows a schematic diagram of the transistor geometries used for the 2D process simulations which were performed using TSUPREM4. Two device geometries were initially simulated, with the dimensions shown along the bottom of the diagram (emitter diameters of 22 and 66 μm). These dimensions were chosen to be consistent with those of $Si_{0.88}Ge_{0.12}$ mesa test transistors for which measured data was available [13, 14]. The measured results were obtained on a device with an emitter dimension of $66 \times 66\ \mu m^2$, and a device comprising nine transistors connected in parallel, each with an emitter geometry of $22 \times 22\ \mu m^2$.

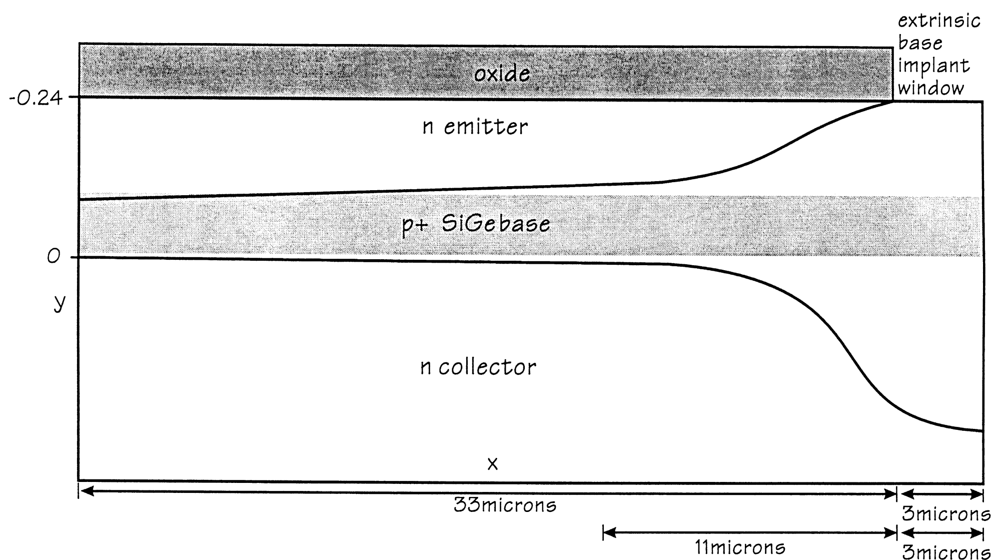

Fig. 1. Schematic illustration of the geometries of the devices studied using the 2D process and device simulations.

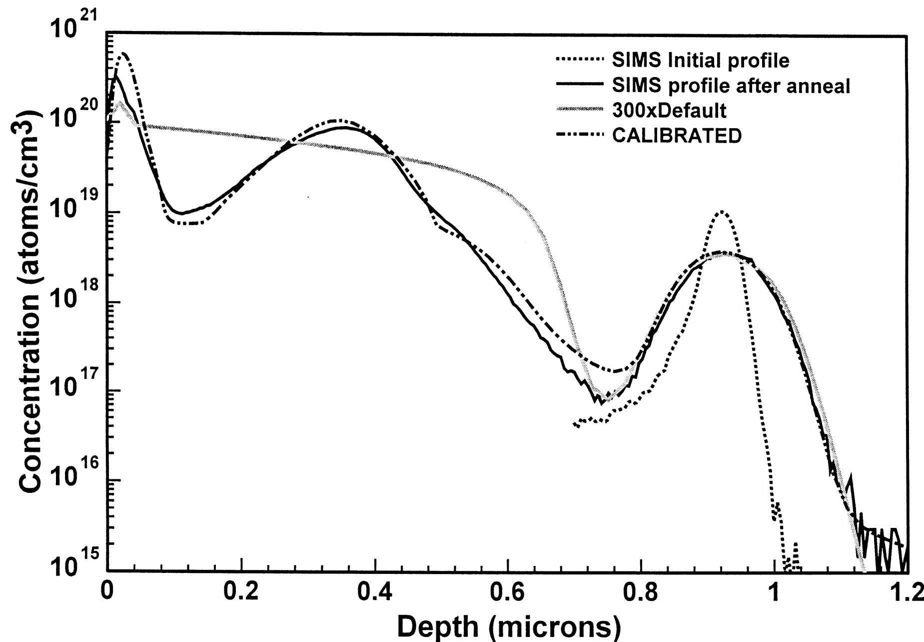

Fig. 2. Comparison of the measured and simulated boron profiles used to calibrate the non-equilibrium diffusion models in the process simulator. The sample was implanted with 120 keV, 2×10^{15} cm^{-2} B and 35 keV, 2×10^{15} cm^{-2} BF_2 and annealed for 30 s at 900°C.

The two experimental devices therefore had the same emitter area of 4356 μm^2, but one had a perimeter of 264 μm and the other a perimeter of 792 μm. The practical devices were fabricated using the process described in Ref. [15] and had an extrinsic base formed from a 120 keV, 2×10^{15} cm^{-2} B implant and a 35 keV, 2×10^{15} cm^{-2} BF_2 implant. The emitter was fabricated using an arsenic-implanted polysilicon emitter contact, and a single anneal of 30 s at 900°C was used to activate the dopant in the extrinsic base and polysilicon emitter.

In order to model diffusion in the SiGe base, it was necessary to modify the diffusion parameters in TSUPREM4 to take into account the slower diffusion of boron in SiGe than Si. In this work, the diffusion coefficient in SiGe was assumed to be four times smaller than that in Si [16]. In the process simulations, Si diffusion parameters were used in the SiGe base, but the thicknesses of the p^+ base and the SiGe spacers were adjusted to take into account the slower diffusion in SiGe than Si. It can readily be shown that a doubling of the width of the p^+ base and a doubling of the undoped SiGe spacer thicknesses is needed to account for the four times lower diffusion coefficient in SiGe than in Si.

The device simulations were carried out using the device simulator MEDICI, and the doping profiles were imported directly from the process simulator. The models used in the simulations for doping induced bandgap narrowing, mobility, and density of states in

Table 1
Summary of the diffusion parameters used in the process simulations

Parameter	Pre-exponent A	Units	B (eV)	Refs.
D_I	1.55×10^6	cm^2 s^{-1}	−3.22	Boit *et al.* ×1.5 [24]
C_I*	3.11×10^{19}	cm^{-3}	−1.58	Boit *et al.* [24]
D_V	6.34×10^3	cm^2 s^{-1}	−3.29	Law [25]
C_V*	4.77×10^{18}	cm^{-3}	−0.71	Law [25]
K_B	1.4	cm^6 s^{-1}	−4	Law [25]
K_{SI}	7.33×10^3	cm × s^{-1}	−1.88	Crowder *et al.* [22]
K_{SV}	1.12×10^4	cm × s^{-1}	−2.48	Law [25]

The parameters are given in the form $A \cdot \exp(B/kT)$.

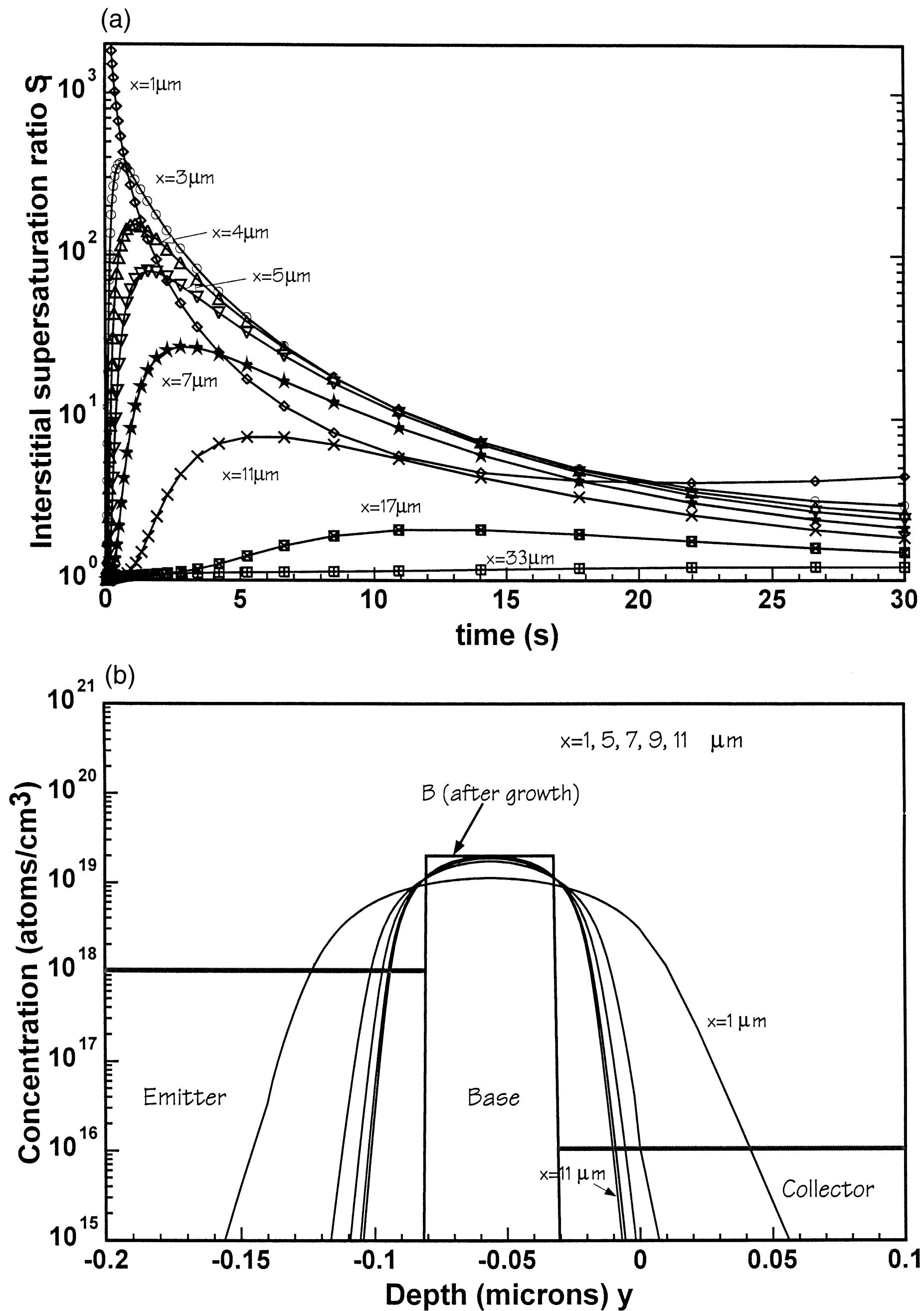

Fig. 3. Effect of a 120 keV, 2×10^{15} cm^{-2} B and 35 keV, 2×10^{15} cm^{-2} BF_2 extrinsic base implant on the boron diffusion at different distances from the edge of the implantation window. (a) Interstitial supersaturation ratio as a function of anneal time at 900°C. (b) Boron profiles after an anneal of 30 s at 900°C.

SiGe were the same as those used in Ref. [13]. The effects of freeze-out were taken into account by calibrating the model to the measured temperature dependence of the base sheet resistance. No attempt has been made to exactly fit the measured and simulated device characteristics, so close agreement between the magnitudes of the measured and simulated currents should not be expected. Nevertheless the trend in the temperature dependences of the measured and simulated collector currents should be broadly similar, since these are determined primarily by the out-diffusion of the boron from the SiGe base.

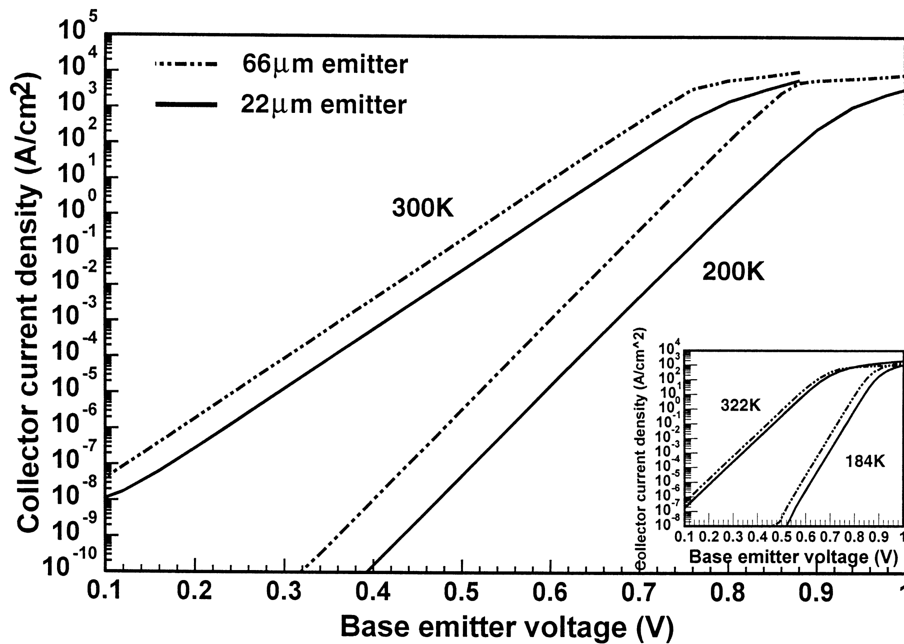

Fig. 4. Simulated collector current densities ($V_{CB} = 0$ V) at temperatures of 300 and 200 K for two $Si_{0.88}Ge_{0.12}$ HBTs with emitter diameters of 22 and 66 μm. For comparison, the inset shows the measured collector current densities on $Si_{0.88}Ge_{0.12}$ HBTs with 5 nm undoped SiGe spacers.

The parameters required to model transient enhanced boron diffusion were calibrated by comparison with measured SIMS profiles on a special test structure in which the extrinsic base implant was made into an *n*-type Si layer above a buried *p*-type Si marker layer. The results are shown in Fig. 2 for the default equilibrium diffusion model and for a full non-equilibrium model. The diffusion coefficient in the default model had to be multiplied by a factor of 300 to give good agreement with the measured boron profile in the marker layer, but this then over-estimated the boron diffusion in the ion implanted region. In contrast, the full non-equilibrium diffusion model is in excellent agreement with the measured profile in both the marker layer and the ion implanted region.

The non-equilibrium model is based around the simplified "plus one" model in which the dose of excess interstitials is directly related to the dose of implanted ions [17, 18]. In our simulations we found that 0.01 excess interstitials per implanted boron ion was required to obtain the fit in Fig. 2. This low ratio is rather surprising, though it should be noted that the assumed dose of 4×10^{13} interstitials cm^{-2} is still very large when it is borne in mind that our background concentration of interstitials at 900°C is only 5×10^{12} cm^{-3}. In addition the $+1$ model tends to imply that the damage cascades from the implanted ions do not overlap, which is not the case for a light element, like boron, implanted at a high dose. The diffusion parameters used in the process simulations are summarised in Table 1 and in Ref. [19] and are essentially similar to those of Lever et al. [20]. Bracht et al. [21] have since published work on zinc diffusion in Si in which a somewhat higher value for D_I and a smaller value for D_V were measured, but the essentials remain unchanged. The three basic quantities on which there appears to be general agreement are $D_I C_I$*, $D_V C_V$* and $K_{SI} C_I$* (or K_{SI}/D_I) and the actual values of D_I, D_V and K_{SI} have to be adjusted to conform to these three quantities if C_I* or C_V* are changed in the input to the program. The value of K_{SI}, the recombination velocity of interstitials at the Si/SiO_2 interface, is particularly important and has been taken from the measurements of Crowder et al. [22]. This parameter determines the extent to which interstitials diffuse laterally from the ion implanted extrinsic base, and hence it has an important influence on the lateral distance over which transient enhanced diffusion occurs. The effective K_{SI} under the boron implants is greatly increased by the expected presence of dislocation loops near the surface as a result of the amorphisation and re-growth caused by the BF_2 implant. We have simulated this effect directly by using the dislocation growth feature in the program. The effect was to essentially maintain the equilibrium value of $C_I = C_I$* at the surface of the implanted regions.

3. Results and discussion

Fig. 3(a) shows the interstitial supersaturation ratio at $y = 0$ (at the depth of the collector/base junction) as a function of anneal time for different lateral distances from the edge of the extrinsic base implant window. In the early stages of the anneal, the interstitial concentration is dramatically increased above its equilibrium value. For example, at a distance of 1 μm from the edge of the extrinsic base implantation window, the interstitial supersaturation ratio peaks at a value of over 1000. As expected, the interstitial concentration decreases on moving laterally away from the edge of the implantation window, but there is still a sizeable enhancement (a factor of nearly 10) at a distance of 11 μm from the implant. At the centre of the device, the interstitial concentration is at its equilibrium value and hence transient enhanced diffusion of the boron would not occur in this part of the base. These simulation results can be understood by considering the parameter values used in Table 1 to model the lateral diffusion of the interstitials. The ratio D_{SI}/K_S can be considered as defining a characteristic "surface diffusion length", which determines the lateral distance over which interstitials diffuse before recombining. From the parameter values in Table 1, the "surface diffusion length" at the anneal temperature of 900°C is 3.7 μm. This value is consistent with the interstitial supersaturation ratios at different depths shown in Fig. 3(a).

Fig. 3(b) shows boron profiles at different lateral distances from the edge of the extrinsic base implant window after an anneal of 30 s at 900°C. Considerable boron diffusion from the base can be seen adjacent to the extrinsic base ($x = 1$ μm), and significant diffusion occurs up to distances of 5 μm from the implant. This result is consistent with the interstitial supersaturation ratios shown in Fig. 3(a).

Fig. 4 shows the simulated collector current densities at temperatures of 300 and 200 K for two $Si_{0.88}Ge_{0.12}$ HBTs with emitter diameters of 22 and 66 μm. For comparison, the inset shows measured collector current densities on $Si_{0.88}Ge_{0.12}$ HBTs with 5 nm undoped SiGe spacers. The main trend identifiable in the simulated characteristics is a lower collector current density for the 22 μm device than the 66 μm device. The difference in collector current density is a factor of approximately 6 at 300 K and 60 at 200 K. A similar trend can be seen in the measured results, though the magnitude of the effect is slightly smaller.

The effects of the boron out-diffusion on the collector current can be seen more clearly in the bandgap narrowing plots shown in Fig. 5(a) and (b) for collector/base reverse biases of 0 and 5 V, respectively. The graphs shown are plots of the ratio of the simulated collector current density J_C to the saturation current density J_O as a function of the reciprocal temperature. The slopes of the graphs give information on the average bandgap narrowing in the base [13]. Results are shown in Fig. 5(a) for two $Si_{0.88}Ge_{0.12}$ HBTs with 66 and 22 μm emitter geometries and for a comparable 66 μm silicon device (i.e. 0% Ge) at a collector/base reverse bias of 0 V. For comparison purposes, the inset shows measured bandgap narrowing plots for two $Si_{0.88}Ge_{0.12}$ HBTs with 5 nm undoped SiGe spacers. The validity of these calculations can be confirmed by referring to the simulated bandgap narrowing plot for the silicon device. An activation energy of 68 meV is obtained, which is in good agreement with the expected value of 70 meV for the doping-induced bandgap narrowing model of Klaassen [23] used in the simulations.

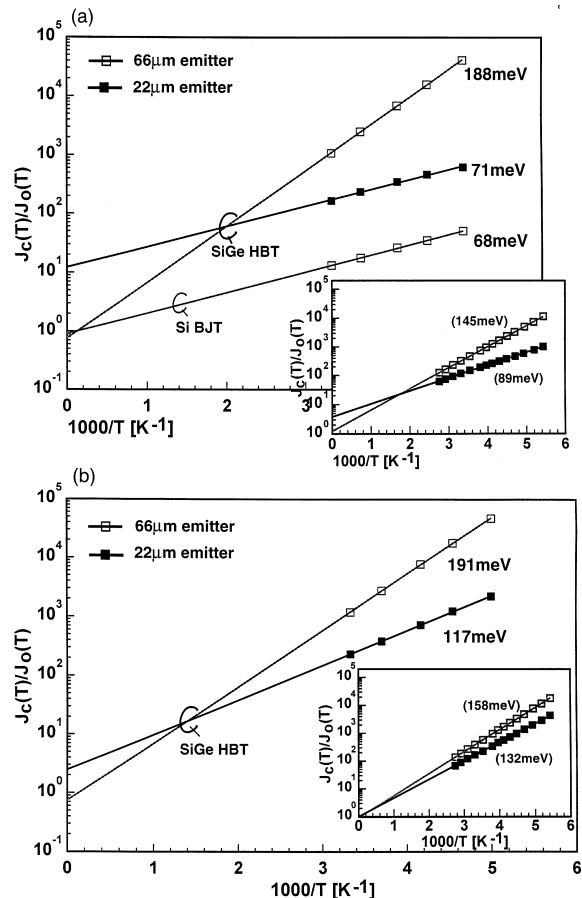

Fig. 5. Plot of the collector current density J_C normalised to the saturation collector current density J_O as a function of reciprocal temperature (bandgap narrowing plots [13, 14]) for two $Si_{0.88}Ge_{0.12}$ HBTs with emitter diameters of 22 and 66 μm. For comparison, the inset shows the measured bandgap narrowing plots on $Si_{0.88}Ge_{0.12}$ HBTs with 5 nm undoped SiGe spacers. (a) Collector/base bias of 0 V. (b) Collector/base reverse bias of 5 V.

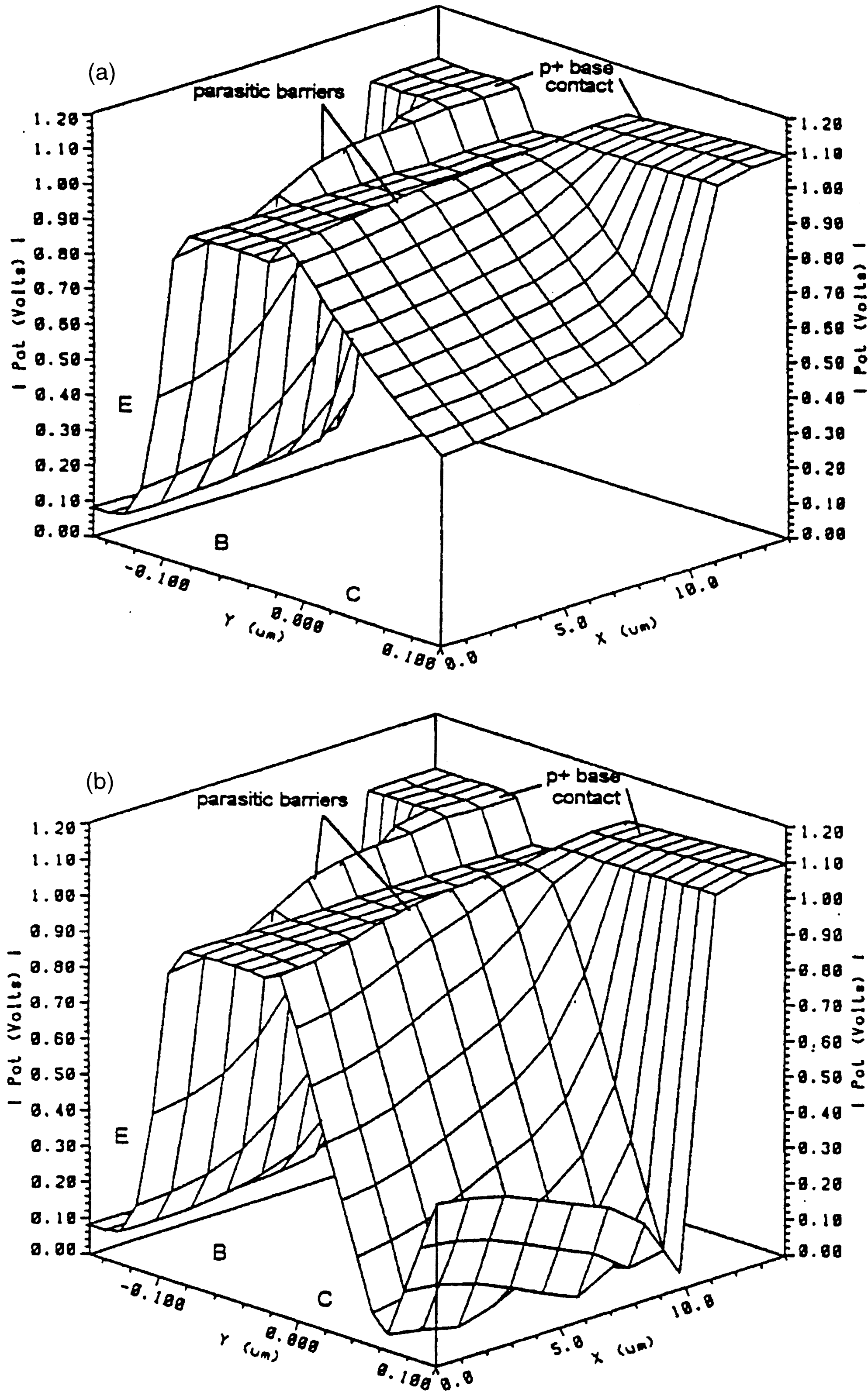

Fig. 6. Plots of the simulated conduction band energy in the x and y directions for a $Si_{0.88}Ge_{0.12}$ HBT with a 22 μm diameter emitter and 5 nm undoped SiGe spacers. (a) Collector/base bias of 0 V. (b) Collector/base reverse bias of 5 V.

For the $Si_{0.88}Ge_{0.12}$ HBTs in Fig. 5(a), activation energies of 188 and 71 meV are predicted for the 66 and 22 μm emitter devices, respectively. A similar, though smaller, change is seen in the measured results in the inset of Fig. 5(a). These results indicate that the simulations are successful in predicting the trend in the measured collector current for transistors with different emitter geometries. Fig. 5(b) shows the effects of an increased collector/base reverse bias of 5 V on the temperature dependence of the collector current. Both simulated and measured characteristics show an increase in activation energy for both 66 and 22 μm emitter devices. This is due to the modulation of the energy barrier at the C/B junction, which is formed as a result of boron out-diffusion from the SiGe base [14]. A comparison of the results in Fig. 5(a) and (b) for the 66 μm device indicates that the simulations predict an increase in activation energy of 3 meV (from 188 to 191 meV) on increasing the C/B bias from 0 to 5 V, which compares with a measured increase of 13 meV (from 145 to 158 meV). For the 22 μm device, the simulations predict an increase of 46 meV (from 71 to 117 meV), which compares with a measured increase of 43 meV (from 89 to 132 meV). This agreement between the measured and simulated results is excellent considering the extreme sensitivity of the collector current to small amounts of boron out-diffusion from the base, and indicates that the "plus one" diffusion model used in this work can successfully predict the trends in the measured collector current.

The effect of the boron out-diffusion on the collector current can be understood by considering the plots of the conduction band energy in Fig. 6(a) and (b) for the 22 μm device at collector/base reverse biases of 0 and 5 V, respectively. Parasitic energy barriers can be seen close to the extrinsic base contact, which get progressively smaller towards the centre of the emitter. These barriers are present at both the emitter/base and collector/base junctions and are due to transient enhanced out-diffusion of boron from the SiGe base at the perimeter of the emitter due to point defects generated by the extrinsic base implant. The penetration of the parasitic energy barrier towards the centre of the emitter is less at the emitter/base junction because the doping concentration in the emitter (1×10^{18} cm^{-3}) is higher than that in the collector (1×10^{16} cm^{-3}). Increasing the collector/base reverse bias from 0 to 5 V has the effect of reducing the extent that the energy barrier at the collector/base junction penetrates towards the centre of the emitter. As a result, the decrease in collector current resulting from the boron out-diffusion is less at higher collector/base reverse biases. The geometry dependence of the collector current arises because the boron out-diffusion takes place over a larger proportion of the emitter area in devices with a smaller emitter size.

Results for thicker 15 nm spacers are shown in Fig. 7(a) for a collector/base bias of 0 V. Both simulated and measured results show increased activation energies for both 22 and 66 μm devices. For the 22 μm device, the simulations predict an increase in activation energy of 107 meV (from 71 to 178 meV) on increasing the spacer width from 5 to 15 nm, which compares with a measured increase of 72 meV (from 89 to 161 meV). For the 66 μm device, the simulations predict an increase of 1 meV (from 188 to 189 meV), which compares with a measured increase of 18 meV (from 145 to 163 meV). Given the extreme sensitivity of the collector current to small amounts of out-diffusion from the SiGe, this agreement between simulated and measured results is reasonable. The simplified "plus one" diffusion model therefore gives a good representation of transient enhanced diffusion in SiGe HBTs. The effect of the 15 nm undoped SiGe spacers on the parasitic energy barriers is indicated in Fig. 7(b) which shows the conduction band energy diagram for a 22 μm emitter device at a collector/base bias of 0 V. A comparison with Fig. 6(a) shows that increasing the undoped SiGe spacer thickness to 15 nm has dramatically reduced the extent that the potential energy barriers penetrate towards the centre of the emitter.

4. Conclusions

Two dimensional process and device simulation has been applied to SiGe HBTs to study the effects of transient enhanced diffusion resulting from point defects generated by an extrinsic base implant. The diffusion simulations were based around a simplified "plus one" model in which the dose of excess interstitials is directly related to the dose of implanted ions. The model was calibrated in 1D by modelling diffusion in a buried boron-doped marker layer below an extrinsic base implant. Good agreement with the measured profile was obtained for a model in which 0.01 excess interstitials were generated per implanted boron ion. 2D process simulations were performed on transistor structures and showed that the point defects generated by the implant caused significant out-diffusion of boron from the SiGe base adjacent to the extrinsic base. A comparison of measured and simulated collector currents was made for SiGe HBTs at temperatures in the range 200–300 K. The collector current was found to vary strongly with device geometry, collector/base voltage and undoped SiGe spacer thickness. The simplified "plus one" transient enhanced diffusion model was able to predict all of the trends in the measured collector current.

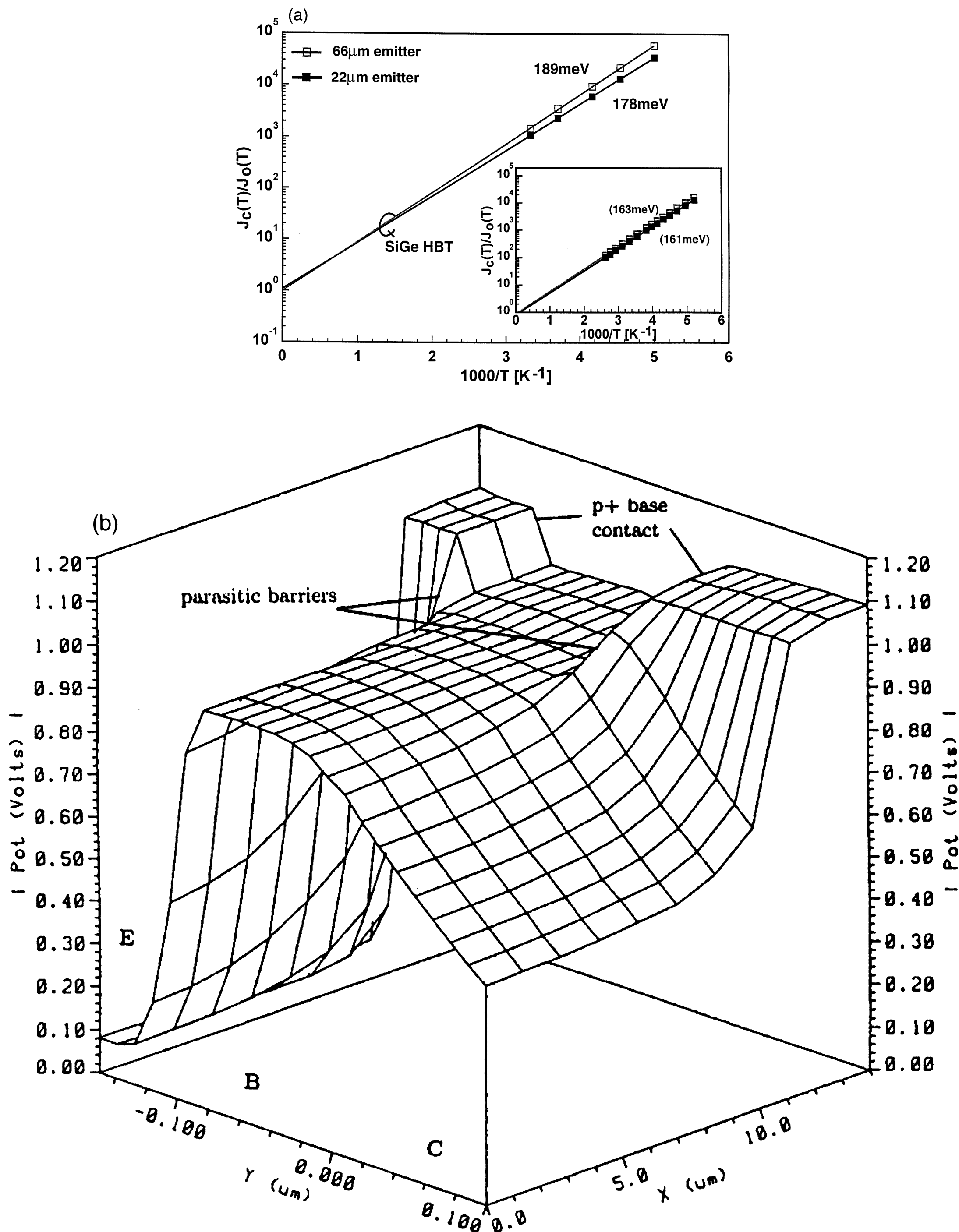

Fig. 7. Electrical characteristics of $Si_{0.88}Ge_{0.12}$ HBTs with a 22 μm emitter and 15 nm undoped SiGe spacers (V_{CB} = 0 V). (a) Simulated and measured (inset) plots of the collector current density J_C normalised to the saturation collector current density J_O as a function of reciprocal temperature (bandgap narrowing plots [13, 14]). (b) Plot of the simulated conduction band energy in the x and y directions.

Acknowledgements

The authors would like to acknowledge the clean room staff at Southampton University for assistance in device fabrication. The research has been carried out with the financial support of EPSRC for device fabrication and of the Universiti Sains Malaysia for the provision of a scholarship.

References

[1] Cuthbertson A, Ashburn P. IEEE Trans Electron Devices 1985;32:2399.
[2] Oda K, Ohue E, Tanabe M, Shimamoto H, Onai T, Washio K. IEDM Technical Digest, 1997:791–94.
[3] Schüppen A, Erben U, Gruhle A, Kibbel H, Schumacher H, König U. IEDM Technical Digest, 1995:743.
[4] Meister T, Shäfer H, Franosch M, Molzer W, Aufinger K, Scheler U, Walz C, Stolz M, Boguth S, Böck J. IEDM Technical Digest, 1995:739.
[5] Pruijmboom A, Terpstra D, Timmerling C, de Boer W, Theunissen M, Slotboom J, Hueting R, Hageraats J. IEDM Technical Digest, 1995:747.
[6] Washio K, Ohue E, Oda K, Tanabe M, Shimamoto H, Onai T. IEDM Technical Digest, 1997:795–98.
[7] de Berranger E, Bodnar S, Chantre A, Kirtsch J, Monroy A, Laurens M, Granier A, Regolini JL, Mouis M. Proc. European Solid State Device Research Conference, 1996:433–36.
[8] Solmi S, Baruffaldi F, Canteri R. J Appl Phys 1991;69:2135.
[9] Cowern NEB, van de Walle GFA, Zalm PC, Vandenhoudt DWE. Appl Phys Lett 1994;65:2981.
[10] Chao HS, Crowder SW, Griffin PB, Plummer JD. JAP 1996;79:2352.
[11] van Dort MJ, van der Wel W, Slotboom JW, Cowern N. EB, Knuvers MPG, Lifka H, Zalm PC. IEDM Technical Digest, 1994:865.
[12] Denorme S, Mathiot D, Dollfus P, Mouis M. IEEE Trans Electron Devices 1995;42:523.
[13] Ashburn P, Boussetta H, Hashim MdR, Chantre A, Mouis M, Parker GJ, Vincent G. IEEE Trans Electron Devices 1996;43:774.
[14] Le Tron B, Hashim MDR, Ashburn P, Mouis M, Chantre A, Vincent G. IEEE Trans Electron Devices 1997;44:715.
[15] Shafi ZA, Gibbings CJ, Ashburn P, Post IRC, Tuppen CG, Godfrey DJ. IEEE Trans Electron Devices 1991;38:1973.
[16] Kuo P, Hoyt JL, Gibbons JF, Mat. Res. Soc., 1995:373.
[17] Jaraiz M, Gilmer GH, Poate JM, de la Rubia TD. Appl Phys Lett 1996;68:409.
[18] Giles MD. J Electrochem Soc 1991;138:1160.
[19] Hashim MdR. Low temperature characterisation of Si bipolar junction transistors and SiGe heterojunction bipolar transistors. Ph.D. thesis, University of Southampton, 1997.
[20] Lever RF, Griffin PB, Rausch WA. J Appl Phys 1995;78:3115.
[21] Bracht H, Stolwijk NA, Mehrer H. Phys Rev B 1995;52:542.
[22] Crowder SW, Hsieh CJ, Griffin PB, Plummer JD. J Appl Phys 1994;76:2756.
[23] Klaassen DBM, Slotboom JW, DeGraaff HC. Solid State Electron 1992;35:125.
[24] Boit C, Lau F, Sittig R. Appl Phys A 1990;50:197.
[25] Law ME. IEEE Trans Comput Aided Des 1991;10:1125.